Two Elementary Problems of Shell Deformation in Plasticity

IOANNIS DOLTSINIS
University of Stuttgart
Faculty of Aerospace Engineering and Geodesy
Pfaffenwaldring 27, 70569 Stuttgart
GERMANY
doltsinis@isd.uni-stuttgart.de

Abstract: The two problems of plastic deformation of membrane shells dealt with are, the expansion of a spherical shell by internal pressure, and the shaping of a dome out of a circular disk. The first problem is easily accessible to an analytical solution which overcomes the pressure maximum and establishes the relationship between the expanding sphere radius and the pertaining pressure in dependence of the hardening of the material. This case may be considered in some sense introductory to the second problem, where a flat circular disk, clamped along the periphery, is blown by pressure such that a dome is formed. The proposed solution approximates the deforming shell as part of a sphere throughout, establishes the static equilibrium with the forming pressure, observes the peripheral kinematic constraint as well as the isochoric condition in plasticity and makes recourse on the flow characteristic of the material. The resulting nonlinear equations relating pressure and dome height are treated numerically by two nested iteration loops.

Key–Words: Membrane shell, plasticity, sphere expansion, dome forming, analytical approach.

1 Introduction

The fascination of numerical results obtained by computer simulations of steadily increasing sophistication does not prohibit essentially approaching a problem by simplified analysis. In the present case the curiosity for an analytical approach originated while spring lattice models were tested against continuous finite elements in the process of forming a dome [1]. An initially flat circular sheet, clamped along the periphery, deforms under gas pressure such that a dome is formed. The problem was stated as that of a deforming membrane shell of elastic-plastic material with a hardening flow characteristic.

The simplest analytical model assumes the shell as that part of a sphere past the fixed circular hole left by the disk in its plane. Geometry relates the decreasing sphere radius to the dome height while maintenance of volume determines the actual thickness of the shell. Eventually the flow characteristic of the material completes the relation between forming pressure and deformation kinematics as expressed in terms of the evolving dome height. This approximation does not care about the kinematic constraint along the clamped boundary. Stress and strain are as for the spherical membrane shell, the thickness homogeneous. The model actually applied in the present study still approximates the shape as part of a varying sphere, but observes the kinematic constraint along the periphery at the basis of the forming dome. The pressure is in static equilibrium with the meridional stress on account of the different shell thickness at apex and basis. The state of stress and strain at the apex is as for the spherical shell just of relevance, at the basis the circumferential strain component is suppressed and the associated vanishing of the deviatoric stress completes there the determination of the stress state. The resulting nonlinear equations governing the pressure as a function of the dome height are treated numerically by two nested iteration loops; their linearized version provides the consecutive algorithm with starting values. The results are not in far distance from the computer simulation using a finite element discretization.

As a precursor to the dome problem, the elementary case of a spherical shell expanding under internal pressure [2] is considered beyond the plastic limit [3]. Particular attention is paid to the pressure maximum, actually experienced when blowing a balloon, and to the associated radius of the sphere as related to the hardening characteristic of the material in plasticity.

The remainder of this communication is as follows: Section 2 deals with the expanding spherical shell, Section 3 developes the solution for the dome forming and the concluding Section 4 summarizes essentials. Regarding the wider basis of the subjects touched in the study refer to [4, 5] for the shell theory, to [6] for the plastic limit and to [7] for instabilities.

2 Expansion of Spherical Membrane Shell

2.1 Failure at plastic limit

The spherical membrane shell of radius r and thickness t is subjected to internal pressure p, Fig. 1. The work rate of the pressure on an expansion of the radius at the rate $\dot{r}$ is

$$L = pS\dot{r}, \tag{1}$$

where S denotes the surface area of the sphere. The yield stress σ_s of the material determines along with the equivalent plastic strain rate $\dot{\bar{\eta}}$ the dissipation rate

$$D = \sigma_s \dot{\bar{\eta}} St. \tag{2}$$

The equivalent strain rate turns out to be equal to the magnitude of the strain rate across the thickness of the membrane shell which is negative while the sphere expands

$$\dot{\bar{\eta}} = \left| \frac{\dot{t}}{t} \right| = -\frac{\dot{t}}{t}. \tag{3}$$

Since plastic deformation does not change the material volume

$$\mathrm{d}(St) = \mathrm{d}(4\pi r^2 t) = 0 \;\Rightarrow\; \frac{\dot{t}}{t} = -2\frac{\dot{r}}{r}. \tag{4}$$

On account of eqn (3) and eqn (4) in eqn (2), the safe load multiplier, the safety factor n, is obtained as

$$n = \frac{D}{L} = \frac{2t\sigma_s}{pr}, \tag{5}$$

which assumes that the pressure in eqn (1) works on the yield mechanism that induces the plastic straining entering the dissipation rate in eqn (2). The limit pressure p_s pertains to $n = 1$:

$$p_s = \frac{2t}{r}\sigma_s. \tag{6}$$

2.2 Beyond the plastic limit

The spherical membrane shell is a statically determinate system that cannot sustain the pressure beyond the limit load as long as the yield stress of the material is insensitive to the deformation as in perfect plasticity. Inspection of eqn (6) confirms this argument even on account of the deforming geometry. The following considers a hardening material with the flow stress σ_f interpreted in terms of the equivalent measures $\bar{\sigma}$ and $\bar{\eta}$ as

$$\bar{\sigma} = \sigma_f(\bar{\eta}). \tag{7}$$

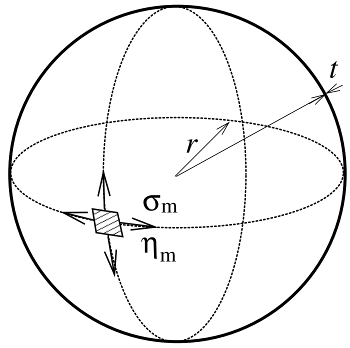

Figure 1: Spherical membrane shell expanding under internal pressure.

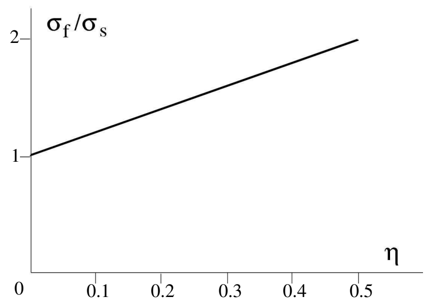

Figure 2: Flow stress of the sheet material.

Static equilibrium with the bi-axial state of membrane stress σ_m, equal along meridians, determines the pressure

$$p = \frac{2t}{r}\sigma_m = \frac{2t}{r}\sigma_f(\bar{\eta}), \tag{8}$$

which implies the equality $\bar{\sigma} = \sigma_m$.

With regard to the pressure maximum eqn (8) is differentiated

$$\frac{\mathrm{d}p}{p} = \frac{\mathrm{d}\sigma_f}{\sigma_f} + \frac{\mathrm{d}t}{t} - \frac{\mathrm{d}r}{r}. \tag{9}$$

From eqn (4),

$$\frac{\mathrm{d}t}{t} = -2\frac{\mathrm{d}r}{r}. \tag{10}$$

Also,

$$\mathrm{d}\sigma_f = \frac{\mathrm{d}\sigma_f}{\mathrm{d}\bar{\eta}}\mathrm{d}\bar{\eta} = -\sigma_f'\frac{\mathrm{d}t}{t} = 2\sigma_f'\frac{\mathrm{d}r}{r}. \tag{11}$$

Using eqn (10) and eqn (11) in eqn (9),

$$\frac{\mathrm{d}p}{p} = 2\left(\frac{\sigma_f'}{\sigma_f} - \frac{3}{2}\right)\frac{\mathrm{d}r}{r}. \tag{12}$$

It follows that an expanding radius of the sphere can be associated to an increasing or to a decreasing pressure

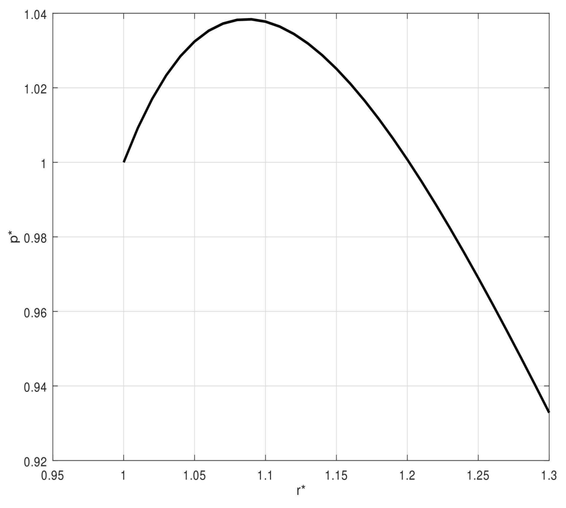

Figure 3: Variation of expansion pressure $p* = (p/p_{\rm s})$ with increasing sphere radius $r* = (r/r_0)$ for $\alpha = 2$.

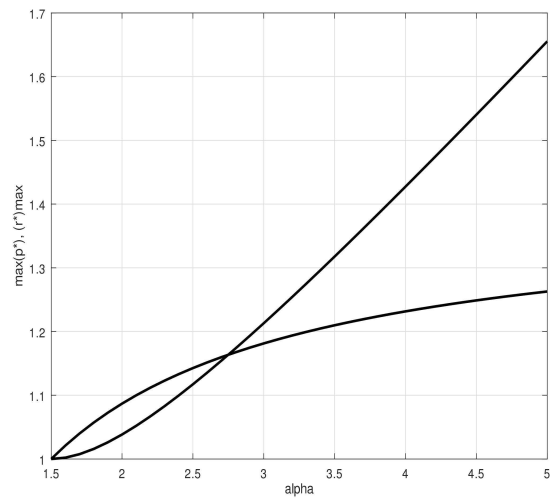

Figure 4: Dependence of maximum pressure $\max(p*) = \max(p/p_{\rm s})$ on the hardening coefficient α (upper) and pertaining radius $(r*)\max = (r/r_0)\max$ (lower).

$$\frac{{\rm d}p}{p} > 0 \quad \text{for} \quad \frac{\sigma_{\rm f}'}{\sigma_{\rm f}} > \frac{3}{2},$$
$$\frac{{\rm d}p}{p} = 0 \quad \text{for} \quad \frac{\sigma_{\rm f}'}{\sigma_{\rm f}} = \frac{3}{2},$$
$$\frac{{\rm d}p}{p} < 0 \quad \text{for} \quad \frac{\sigma_{\rm f}'}{\sigma_{\rm f}} < \frac{3}{2}, \qquad (13)$$

which indicates the maximum at $\sigma_{\rm f}'/\sigma_{\rm f} = 3/2$. The pressure can be augmented as long as $\sigma_{\rm f}'/\sigma_{\rm f} > 3/2$, and it has to be diminished when $\sigma_{\rm f}'/\sigma_{\rm f} < 3/2$.

A standardized fashion of eqn (8) reads

$$\frac{p}{p_{\rm s}} = \frac{t}{t_0}\frac{r_0}{r}\frac{\sigma_{\rm f}(\bar{\eta})}{\sigma_{\rm s}}, \quad p_{\rm s} = \frac{2t_0}{r_0}\sigma_{\rm s}, \qquad (14)$$

where $p_{\rm s}$ is the pressure at incipient yield computed for the original geometry r_0, t_0 of the membrane shell. The maintenance of volume during the course of plastic deformation is expressed by

$$\frac{St}{S_0 t_0} = \frac{4\pi r^2 t}{4\pi r_0^2 t_0} = 1 \;\Rightarrow\; \frac{t}{t_0} = \frac{r_0^2}{r^2}, \qquad (15)$$

in agreement with eqn (4). Furthermore, the equivalent strain can be expressed in terms of the thickness strain (cf eqn (3)) and with eqn (15),

$$\bar{\eta} = -\eta_{\rm t} = -\ln\frac{t}{t_0} = 2\ln\frac{r}{r_0}. \qquad (16)$$

Once the functional dependence $\sigma_{\rm f}(\bar{\eta})$ of the material flow stress is available, eqn (14) along with eqn (15) for the thickness and eqn (16) for the equivalent plastic strain determine the pressure as a function of the expanding radius. In order to be specific the sheet material is assumed obeying a linearly hardening flow stress, (Fig. 2):

$$\sigma_{\rm f} = \sigma_{\rm s}(1 + \alpha\bar{\eta}), \qquad (17)$$

where $\sigma_{\rm s}$ denotes the initial yield stress and the coefficient α rules the hardening. This gives the pressure as

$$\frac{p}{p_{\rm s}} = \left(\frac{r}{r_0}\right)^{-3}\left(1 + 2\alpha\ln\frac{r}{r_0}\right). \qquad (18)$$

The variation of the pressure in the sphere with increasing radius is plotted in Fig. 3 for the hardening coefficient $\alpha = 2$. The radius at maximum pressure is determined from the condition for the flow stress in eqn (13) in terms of eqn (17) as

$$\left.\frac{r}{r_0}\right|_{\max} = \exp\left(\frac{2\alpha - 3}{6\alpha}\right). \qquad (19)$$

With this in eqn (18) the pressure maximum becomes

$$\max\left(\frac{p}{p_{\rm s}}\right) = \frac{2\alpha}{3}\left.\frac{r}{r_0}\right|_{\max}^{-3} = \frac{2\alpha}{3}\exp\left(\frac{3 - 2\alpha}{2\alpha}\right). \qquad (20)$$

The variation of the maximum pressure and of the pertaining radius with the hardening coefficient α is depicted in Fig. 4.

It is worth notice by inspection of eqn (19) that the radius at the pressure maximum does not exceed the mark of $r/r_0 = \exp(1/3) = 1.3956$ as long as

$\alpha > 0$. Instead of the linear hardening statement, the flow stress of the material is frequently described by the power law

$$\sigma_{\rm f} = \sigma_{\rm s}\bar{\eta}^m, \tag{21}$$

where $m = 0$ signifies perfect plasticity: $\sigma_{\rm f} = \sigma_{\rm s} =$ constant. The pressure maximum is for

$$\frac{\sigma_{\rm f}'}{\sigma_{\rm f}} = \frac{m}{\bar{\eta}} = \frac{3}{2}, \tag{22}$$

which gives the pertaining radius

$$\left.\frac{r}{r_0}\right|_{\max} = \exp\left(\frac{\bar{\eta}}{2}\right) = \exp\left(\frac{m}{3}\right). \tag{23}$$

For the limiting value $m = 1$ of the exponent: $r/r_0 = 1.3956$.

3 Plastic Forming of Dome

3.1 Definition of problem

The flat circular sheet in Fig. 5 (radius A, homogeneous thickness t_0) is clamped along the periphery and is subjected to gas pressure such that it assumes the shape of a dome. The sheet material is assumed plastic with a linearly hardening characteristic as in eqn (17) with $\alpha = 2$ in the numerical evaluation.

The evolving shell with distributed sheet thickness t is considered part of a sphere of radius r and height h, both varying during the course of the deformation process and related by

$$\frac{r}{A} = \frac{A^2 + h^2}{2hA} = \frac{1 + y^2}{2y}. \tag{24}$$

The quantity

$$y = \frac{h}{A} \tag{25}$$

introduces a dimensionless variable for the height h while A is fixed. The surface area S of the spherical dome at height h as compared to the area of the flat sheet is

$$\frac{S}{\pi A^2} = \frac{2\pi r h}{\pi A^2} = \frac{A^2 + h^2}{A^2} = 1 + y^2. \tag{26}$$

3.2 Approximate analysis

The kinematic constraint along the periphery at the basis b of the shell suggests a distinction to the apex a. Stress and strain at the apex a are as for a spherical membrane shell; at the basis b the circumferential strain is suppressed (Fig. 5). The forming pressure is equilibrated by the meridional stress in the assumed spherical membrane shell. On account of different sheet thicknesses at apex and basis,

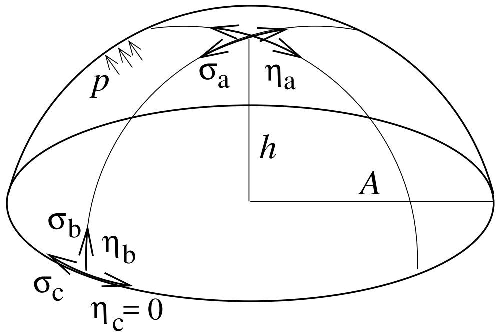

Figure 5: Deforming membrane shell. Geometry, stress and strain.

$$p = \frac{2}{r}t_{\rm a}\sigma_{\rm a} = \frac{2}{r}t_{\rm b}\sigma_{\rm b}. \tag{27}$$

The membrane stress state at the apex comprises the meridional components $\sigma_{\rm a}, \sigma_{\rm a}$, the equivalent stress is

$$\bar{\sigma}_{\rm a} = \sigma_{\rm a}. \tag{28}$$

The suppressed circumferential plastic strain at the basis implies vanishing of the associated deviatoric stress. The induced circumferential stress is $\sigma_{\rm b}/2$, half of the meridional stress $\sigma_{\rm b}$. The equivalent stress is

$$\bar{\sigma}_{\rm b} = \frac{\sqrt{3}}{2}\sigma_{\rm b}. \tag{29}$$

Kinematic quantities enter by the flow characteristic of the material, eqn (17). The state of strain at the apex is specified by the meridional components $\eta_{\rm a}, \eta_{\rm a}$; the thickness strain $\eta_{\rm ta} = -2\eta_{\rm a}$ compensates for no change in volume. The equivalent plastic strain is

$$\bar{\eta}_{\rm a} = 2\eta_{\rm a} = -\eta_{\rm ta} = -\ln\frac{t_{\rm a}}{t_0}. \tag{30}$$

Equating the equivalent stress, eqn (28), to the flow stress from the material characteristic, and with eqn (30) for the equivalent strain,

$$\sigma_{\rm a} = \sigma_{\rm s}\left(1 - \alpha\ln\frac{t_{\rm a}}{t_0}\right). \tag{31}$$

At the basis the strain state comprises the meridional component $\eta_{\rm b}$ and the thickness strain $\eta_{\rm tb} = -\eta_{\rm b}$; the circumferential component is suppressed. The equivalent plastic strain is

$$\bar{\eta}_{\rm b} = \frac{2}{\sqrt{3}}\eta_{\rm b} = \frac{2}{\sqrt{3}}(-\eta_{\rm tb}) = -\frac{2}{\sqrt{3}}\ln\frac{t_{\rm b}}{t_0}. \tag{32}$$

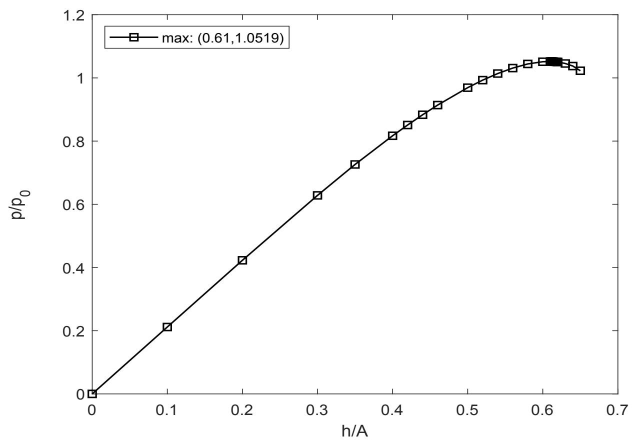

Figure 6: Forming pressure p/p_0 as a function of the dome height h/A.

The pertaining equivalent stress, eqn (29), enters the flow characteristic of the material along with eqn (32) for the equivalent strain

$$\frac{\sqrt{3}}{2}\sigma_{\mathrm{b}} = \sigma_{\mathrm{s}}\left(1 - \frac{2}{\sqrt{3}}\alpha \ln \frac{t_{\mathrm{b}}}{t_0}\right). \quad (33)$$

With σ_{a} from eqn (31) and σ_{b} from eqn (33) in eqn (27) for the pressure, normalization by $p_0 = 2t_0\sigma_{\mathrm{s}}/A$ gives

$$\begin{aligned} \frac{p}{p_0} &= \frac{t_{\mathrm{a}}}{t_0}\left(1 - \alpha \ln \frac{t_{\mathrm{a}}}{t_0}\right)\frac{2y}{1+y^2} \\ &= \frac{2}{\sqrt{3}}\frac{t_{\mathrm{b}}}{t_0}\left(1 - \frac{2}{\sqrt{3}}\alpha \ln \frac{t_{\mathrm{b}}}{t_0}\right)\frac{2y}{1+y^2}, \end{aligned} \quad (34)$$

where the radius of the spherical shell has been expressed using eqn (24). In addition to the above equality the conservation of the shell volume in plastic deformation constrains the sheet thickness. Approximating the deformed volume by

$$\int_s t\mathrm{d}S \approx \frac{t_{\mathrm{a}} + t_{\mathrm{b}}}{2}S = \frac{t_{\mathrm{a}} + t_{\mathrm{b}}}{2}2\pi r h \quad (35)$$

with the shell surface S from eqn (26), the requirement transfers to the average sheet thickness as

$$\begin{aligned} &\frac{\int_s t\mathrm{d}S}{\pi A^2 t_0} = \frac{2\pi r h}{\pi A^2}\frac{1}{2}\left(\frac{t_{\mathrm{a}}}{t_0} + \frac{t_{\mathrm{b}}}{t_0}\right) = 1 \\ \Rightarrow\ &\frac{1}{2}\left(\frac{t_{\mathrm{a}}}{t_0} + \frac{t_{\mathrm{b}}}{t_0}\right) = \frac{A^2}{A^2 + h^2} = \frac{1}{1+y^2}. \end{aligned} \quad (36)$$

This completes the determination of the pressure p/p_0 as a function of the progressing height $y = h/A$ of the dome. An explicit estimate of the solution is obtained by the approximation

$$\ln \frac{t}{t_0} \Leftarrow \left(\frac{t}{t_0} - 1\right)\frac{t_0}{t} = \frac{t - t_0}{t}, \quad (37)$$

which replaces in fact the logarithmic strain by the thickness reduction per actual sheet thickness. Thereby the equality requirement for the meridional traction at apex and basis from eqn (34) simplifies to

$$\begin{aligned} &\frac{\sigma_{\mathrm{a}} t_{\mathrm{a}}}{\sigma_{\mathrm{s}} t_0} \Leftarrow (1-\alpha)\frac{t_{\mathrm{a}}}{t_0} + \alpha = \\ &= \frac{2}{\sqrt{3}}\left(1 - \frac{2\alpha}{\sqrt{3}}\right)\frac{t_{\mathrm{b}}}{t_0} + \frac{4\alpha}{3} \Rightarrow \frac{\sigma_{\mathrm{b}} t_{\mathrm{b}}}{\sigma_{\mathrm{s}} t_0}. \end{aligned} \quad (38)$$

The solution of eqn (38) along with the thickness constraint from eqn (36) is

$$\begin{aligned} \frac{t_{\mathrm{a}}}{t_0} &= \frac{2}{7\alpha - 3 - 2\sqrt{3}}\left(\frac{4\alpha - 2\sqrt{3}}{1+y^2} - \frac{\alpha}{2}\right), \\ \frac{t_{\mathrm{b}}}{t_0} &= \frac{2}{1+y^2} - \frac{t_{\mathrm{a}}}{t_0}. \end{aligned} \quad (39)$$

Using the above results in eqn (34) for the pressure along with the approximation of the logarithm by eqn (37) gives the same result at apex and basis. Of course, the result at the two positions differs if the thickness from the simplified eqn (39) is used in conjunction with the original logarithmic expressions in eqn (34).

A numerical solution of the nonlinear system of eqns (34) and (36) for the sheet thickness at fixed dome height is obtained iteratively as follows

$$\begin{aligned} &\text{Predictor} && \left.\frac{t_{\mathrm{a}}}{t_0}\right|_i \\ &\text{Evaluation} && f\left(\left.\frac{t_{\mathrm{a}}}{t_0}\right|_i\right) = \left.\frac{t_{\mathrm{a}}}{t_0}\right|_i\left(1 - \alpha \ln \left.\frac{t_{\mathrm{a}}}{t_0}\right|_i\right) \\ &\text{Solution} && \frac{2}{\sqrt{3}}\left.\frac{t_{\mathrm{b}}}{t_0}\right|_i\left(1 - \frac{2}{\sqrt{3}}\alpha \ln \left.\frac{t_{\mathrm{b}}}{t_0}\right|_i\right) \\ & && = f\left(\left.\frac{t_{\mathrm{a}}}{t_0}\right|_i\right) \\ &\text{Corrector} && \left.\frac{t_{\mathrm{a}}}{t_0}\right|_{i+1} = \frac{2}{1+y^2} - \left.\frac{t_{\mathrm{b}}}{t_0}\right|_i. \end{aligned} \quad (40)$$

The iteration is started with the linear approximation for t_{a}/t_0 from eqn (39) as an estimate. The solution step in the above scheme activates an interior iteration loop for t_{b}/t_0:

$$\left.\frac{t_{\mathrm{b}}}{t_0}\right|_{k+1} = \exp\left[\frac{\sqrt{3}}{2\alpha} - \frac{3}{4\alpha}f\left(\left.\frac{t_{\mathrm{a}}}{t_0}\right|_i\right)\left.\frac{t_{\mathrm{b}}}{t_0}\right|_k^{-1}\right]. \quad (41)$$

The starting value here is from the linearized fashion of the equation for $(t_{\mathrm{b}}/t_0)_i$ in the scheme owed to the approximation of the logarithm by eqn (37)

$$\left.\frac{t_{\mathrm{b}}}{t_0}\right|_0 = \frac{1}{4\alpha - 2\sqrt{3}}\left[4\alpha - 3f\left(\left.\frac{t_{\mathrm{a}}}{t_0}\right|_i\right)\right]. \quad (42)$$

The sheet thickness values computed consecutively while the height of the dome is augmented enter the evaluation of the pressure by eqn (34). The result for the hardening coefficient $\alpha = 2$ is plotted in Fig 6. The pressure maximum is obtained at

$$\frac{p}{p_0} = 1.0519, \quad \frac{h}{A} = 0.610 \div 0.611.$$

4 Conclusion

The behaviour of two membrane shells deforming plastically under pressure has been studied analytically. The simple solution for the expanding spherical shell is discussed as a precursor to the more demanding problem of forming a dome out of a flat sheet. Of interest, the appearance of the pressure maximum while the sphere expands, as experienced when blowing a balloon, and its dependence on the hardening characteristic of the material.

The dome forming has been accessed by an approximate solution that mainly satisfies the static equilibrium and the kinematic constraints on structure and material. To be specific, the model is founded on the geometrical approximation of the shell shape throughout as part of a shrinking sphere, establishes the static equilibrium for the forming pressure, observes the kinematic constraint along the fixed boundary as well as the isochoric condition of plastic flow and makes recourse on the hardening characteristic of the material. The nonlinear equations governing the system are solved numerically by iteration. The results show that the selected approach to handle the problem is reasonable.

The software packages provided by MATLAB [8] and GNU OCTAVE [9] were helpful in carrying out the numerical operations and producing the associated graphics.

References:

[1] I. Doltsinis, M. Reck and V. Dias da Silva, Spring lattice models in the nonlinear analysis of shells – an applicability study in elasticity, plasticity and damage, *CST 2018, Barcelona, Spain, 4-6 September 2018*, to be published 2019.

[2] I. Doltsinis, *Elements of Plasticity*, WIT Press, Southampton, 2000.

[3] I. Doltsinis, Plastic limit of structures and energy principles, *Archives of Computational Methods in Engineering* 24, 2017, pp. 165–187.

[4] S. Timoshenko and S. Woinowsky-Krieger, *Theory of Plates and Shells*, 2nd Edition, McGraw-Hill, New York, 1959.

[5] W. Flügge, *Stresses in Shells*, Springer, Berlin, 1960.

[6] W.T. Koiter, General theorems for elastic–plastic solids, in I.N. Sneddon and R. Hill (Eds.), *Progress in Solid Mechanics*, Vol. 1, Chapter 4, North-Holland, Amsterdam, 1960.

[7] H. Petryk (Ed.), *Material Instabilities in Elastic and Plastic Solids*, CISM Courses and Lectures No. 414, Springer, Wien, New York, 2000.

[8] MATLAB The Language of Technical Computing, The MathWorks, Inc., https://de.mathworks.com/products/matlab.html

[9] J. W. Eaton, D. Bateman, S. Hauberg and R. Wehbring, GNU Octave version 3.8.1 manual: a high-level interactive language for numerical computations, CreateSpace Independent Publishing Platform, ISBN 1441413006, 2014. www.gnu.org/software/octave/doc/interpreter/